

## The Role of Bromide Ions in Seeding Growth of Au Nanorods

Niti Garg, Clark Scholl, Ashok Mohanty, and Rongchao Jin\*

Department of Chemistry, Carnegie Mellon University, Pittsburgh, Pennsylvania 15213

Received January 29, 2010. Revised Manuscript Received March 23, 2010

We report our findings on the important role of bromide ions in the seeding growth process of Au nanorods. The seed-mediated process constitutes a well-developed method for synthesizing gold nanorods in high yield, which is facilitated by a micelle-forming surfactant, cetyltrimethylammonium bromide (CTA-Br). Despite the tremendous work in recent years, the growth mechanism of Au nanorods has not been fully understood. Contrary to the widely accepted mechanism of CTA<sup>+</sup> micelle-templated growth of Au nanorods, we have identified the critical role of bromide ions in the seeding growth of Au nanorods. We found that even when the micelle-forming agent (CTA<sup>+</sup>) concentration is below its critical micelle concentration (cmc), bromide ions added in the form of NaBr can successfully effect the growth of Au nanorods in good yield. By controlling the concentration of externally added bromide ions, the rod shape and dimensions of the resulting Au nanoparticles can be readily controlled in the presence of only a minimum amount of CTABr (as a steric stabilizer for nanorods). High-resolution TEM studies show that the as-formed nanorods are perfectly single crystalline, instead of penta-twinned ones, and are bound by {111} and {100} facets with a [110] direction as the elongation direction. A mechanism is proposed to account for the seeding growth of single crystalline Au nanorods. Overall, this work explicitly demonstrates that Br<sup>-</sup> indeed serves as an important shape-directing agent for gold nanorod formation in the seed-mediated process.

## 1. Introduction

Noble metal nanoparticles exhibit interesting optical properties originated from excitation of free electrons in the particle (i.e., surface plasmon resonance, SPR).<sup>1–8</sup> The plasmon excitation gives rise to strong light absorption, scattering, and optical near-fields, the latter being particularly important for surface-enhanced Raman scattering of adsorbed molecules on the particle surface.<sup>8</sup> The surface plasmon modes of metal nanoparticles are determined by particle size, shape, and particle-to-particle interaction.<sup>9–20</sup> Although spherical particles can be readily

synthesized, the tunability of the SPR of nanospheres is, however, limited;<sup>21</sup> for example, spherical Au particles ranging from 10 to 100 nm (diameter) only show a moderate tunability of SPR wavelength by ~50 nm ( $\lambda_{\text{peak}}$  varying from ~520 to ~570 nm). On the other hand, nonspherical (i.e., anisotropic) particles are much more efficient in this aspect due to their extreme sensitivity to factors such as particle shape (e.g., nanorods), the shape anisotropy (e.g., aspect ratio of nanorods), and tip truncation (e.g., the case of nanoprisms).<sup>22–25</sup> For Au nanorods, a slight change in aspect ratio from ~2.5 to ~3 can lead to a 50 nm red shift of the longitudinal plasmon mode, equivalent to the maximum SPR tunability of Au nanospheres. The high efficiency of nanorods in terms of SPR tunability is also reflected in that the nanorod's volume increases only by a factor of 1.2 while the spherical particle's volume changes by 1000 times when going from 10 to 100 nm (diameter) in order to achieve the 50 nm tunability.

Thus, far, there have been a variety of anisotropic nanoparticles, such as nanocubes, nanoprisms, nanorods, and nanowires, etc.<sup>26–29</sup> Their optical absorption or scattering wavelengths cover the entire visible spectrum, even up to the near-infrared spectral range. Among these nanostructures, the rod-shaped nanoparticles are the earliest explored (back to late 1990s). Their optical properties are mainly controlled by the length and are insensitive to the rod diameter.<sup>2,5,22</sup> Thus, simply by controlling the rods' aspect ratio (length-to-diameter ratio) in the synthesis, one can readily obtain any color in the visible range, which renders Au

\*Corresponding author. E-mail: rongchao@andrew.cmu.edu.

(1) Wei, W.; Li, S.; Qin, L.; Xue, C.; Millstone, J. E.; Xu, X.; Schatz, G. C.; Mirkin, C. A. *Nano Lett.* **2008**, *8*, 3446–3449.

(2) Murphy, C. J. *ACS Nano* **2009**, *3*, 770–774.

(3) Tabor, C.; Van Haute, D.; El-Sayed, M. A. *ACS Nano* **2009**, *3*, 3670–3678.

(4) Wiley, B.; Sun, Y.; Xia, Y. *Acc. Chem. Res.* **2007**, *40*, 1067–1076.

(5) Yu, Y.-Y.; Chang, S.-S.; Lee, C.-L.; Wang, C. R. C. *J. Phys. Chem. B* **1997**, *101*, 6661–6664.

(6) Gao, H.; Henzie, J.; Odom, T. W. *Nano Lett.* **2006**, *6*, 2104–2107.

(7) Ni, W.; Ambrjansson, T.; Apell, S. P.; Chen, H.; Wang, J. *Nano Lett.* **2010**, *10*, 77–84.

(8) Dieringer, J. A.; Wustholz, K. L.; Masiello, D. J.; Camden, J. P.; Kleinman, S. L.; Schatz, G. C.; Van Duyne, R. P. *J. Am. Chem. Soc.* **2009**, *131*, 849–854.

(9) Chang, S.-S.; Shih, C.-W.; Chen, C.-D.; Lai, W.-C.; Wang, C. R. C. *Langmuir* **1999**, *15*, 701–709.

(10) Hubert, F.; Testard, F.; Spalla, O. *Langmuir* **2008**, *24*, 9219–9222.

(11) Jin, R.; Cao, Y. W.; Mirkin, C. A.; Kelly, K. L.; Schatz, G. C.; Zheng, J. G. *Science* **2001**, *294*, 1901–1903.

(12) Jin, R.; Cao, Y. C.; Hao, E.; Métraux, G. S.; Schatz, G. C.; Mirkin, C. A. *Nature* **2003**, *425*, 487–490.

(13) Liu, M.; Guyot-Sionnest, P. *J. Phys. Chem. B* **2004**, *108*, 5882–5888.

(14) Perez-Juste, J.; Pastoriza-Santos, I.; Liz-Marzan, L. M.; Mulvaney, P. *Coord. Chem. Rev.* **2005**, *249*, 1870–1901.

(15) Lu, X.; Tuan, H.-Y.; Chen, J.; Li, Z.-Y.; Korgel, B. A.; Xia, Y. *J. Am. Chem. Soc.* **2007**, *129*, 1733–1742.

(16) Burgin, J.; Liu, M.; Guyot-Sionnest, P. *J. Phys. Chem. C* **2008**, *112*, 19279–19282.

(17) Hill, H. D.; Millstone, J. E.; Banholzer, M. J.; Mirkin, C. A. *ACS Nano* **2009**, *3*, 418–424.

(18) Smith, D. K.; Miller, N. R.; Korgel, B. A. *Langmuir* **2009**, *25*, 9518–9524.

(19) Kawasaki, H.; Nishimura, K.; Arakawa, R. *J. Phys. Chem. C* **2007**, *111*, 2683–2690.

(20) Khalavka, Y.; Becker, J.; Sonnichsen, C. *J. Am. Chem. Soc.* **2009**, *131*, 1871–1875.

(21) Daniel, M.-C.; Astruc, D. *Chem. Rev.* **2004**, *104*, 293–346.

(22) Eustis, S.; El-Sayed, M. *J. Phys. Chem. B* **2005**, *109*, 16350–16356.

(23) Jena, B. K.; Raj, C. R. *J. Phys. Chem. C* **2007**, *111*, 15146–15153.

(24) Yoo, H.; Millstone, J. E.; Li, S.; Jang, J.-W.; Wei, W.; Wu, J.; Schatz, G. C.; Mirkin, C. A. *Nano Lett.* **2009**, *9*, 3038–3041.

(25) Ming, T.; Feng, W.; Tang, Q.; Wang, F.; Sun, L.; Wang, J.; Yan, C. *J. Am. Chem. Soc.* **2009**, *131*, 16350–16351.

(26) Xia, Y.; Xiong, Y.; Lim, B.; Skrabalak, S. E. *Angew. Chem., Int. Ed.* **2009**, *48*, 60–103.

(27) Liu, M.; Guyot-Sionnest, P. *J. Mater. Chem.* **2006**, *16*, 3942–3945.

(28) Liz-Marza'n, L. M. *Langmuir* **2006**, *22*, 32–41.

(29) Link, S.; El-Sayed, M. A. *Annu. Rev. Phys. Chem.* **2003**, *54*, 331–366.

nanorods of particular interest for biological and biomedical applications since color-based imaging and tracking are essential in these applications. With respect to the synthetic protocols of Au nanorods, Murphy and co-workers<sup>30</sup> developed a facile seed-mediated method for synthesizing Au nanorods involving cetyltrimethylammonium bromide (CTABr). Although this process has now become a standard protocol for nanorod synthesis,<sup>30,31</sup> the factors responsible for shape control are still elusive. The synthetic procedure involves two main steps.<sup>30,31</sup> In the first step, metal salt (e.g., HAuCl<sub>4</sub>) is reduced with a strong reducing agent (e.g., sodium borohydride) in the presence of a stabilizing agent (citrate or CTABr) to yield 2–4 nm quasi-spherical Au seeds. In the next step, the seeds are added to a growth solution containing metal salt, weak reducing agent (ascorbic acid), and CTABr, and Au nanorods are produced by 1D seeding growth; note that addition of AgNO<sub>3</sub> increases the nanorod yield but restricts the attainable aspect ratio.<sup>32</sup> In their initial report, Jana et al. used citrate-stabilized seeds and the nanorod yield was not high (~15%).<sup>30</sup> Later, Nikoobakht et al. modified the approach by using CTABr-stabilized Au seeds and increased the nanorod yield to ~100%.<sup>31</sup> The aspect ratio of nanorods is found to vary significantly with the amount of AgNO<sub>3</sub> in the growth solution. Au nanorods of high aspect ratio (~25) could be achieved in the absence of Ag<sup>+</sup> but with low yield, whereas in the presence of Ag<sup>+</sup> the aspect ratio achievable is typically < 6 but with high yield.<sup>32</sup>

Many efforts have been made to understand the mechanism of the growth process. Particularly, the roles of the seeds, Ag<sup>+</sup> ions, and CTABr concentration have been investigated systematically.<sup>32–38</sup> The results of these studies can be summarized as follows. The role of the seeds is to induce face-selective deposition of Au(0) and hence anisotropic growth. HR-TEM studies have indicated that the CTABr-capped seeds used for nanorod growth are single crystalline with well-developed facets.<sup>35</sup> The role of Ag<sup>+</sup> is to selectively adsorb onto Au {110} facets by underpotential deposition (UPD) and hence to direct Au deposition on {100} and {111} surfaces, leading to nanorod growth in the [100] direction.<sup>35</sup> In the absence of Ag<sup>+</sup> ions, the nanorods grow via a somewhat different mechanism, i.e., in the [110] direction.<sup>34–36</sup> The role of CTABr is a subject of debate in the literature and has not been well understood.<sup>37</sup> The popular perception is that the rodlike micelles of CTABr act as a soft template for Au nanorod growth.<sup>29–35</sup> But this does not explain why a very high concentration of CTABr (0.1 M) is needed for nanorod growth; note that the critical micellar concentration (cmc) of CTABr is far less (~1 mM). It is generally accepted that CTA<sup>+</sup> stabilizes the nanorods by forming a bilayer around the nanorod.<sup>2,31</sup> If this is the only role of CTABr in Au nanorod growth, the use of CTA-Cl should also result in formation of Au nanorods. But literature reports<sup>32,39</sup> as well as our own observation indicate that when CTA-Cl is used, only spherical particles are formed. This led us to suspect that the counterion (Br<sup>-</sup>) in CTA-Br has a profound effect on the nanorod formation process. Of note, the important

role of anions in Pd, Ag, and Cu nanocrystal growth has been reported.<sup>4,40</sup> Also, in the case of Au nanorod growth, it has been shown that the presence of a very low amount of iodide impurity in CTA-Br significantly disrupts the formation of nanorods.<sup>18</sup> Overall, it is highly desirable to investigate whether bromide ion has any role in the Au nanorod growth process.

Herein, we report our systematic studies on the major role of bromide ions in the seeding growth of Au nanorods. Bromide ions are simple ions and are not thought to be a shape-directing agent. However, in our work we found that bromide ions actually induce the formation of Au nanorods, even when the CTA-Br concentration is below its cmc. Thus, the role of CTA-Br micelles as a soft template for Au nanorod growth is less significant, albeit it cannot be completely ruled out based upon our current data. The high concentration of CTA-Br needed for Au nanorod growth is indeed due to the need for high concentration of bromide ions, and the role of CTA<sup>+</sup> ions is to sterically stabilize the nanorods by the formation of bilayers on nanorods.

## 2. Materials and Methods

**2.1. Materials.** Hydrogen tetrachloroaurate (HAuCl<sub>4</sub>·3H<sub>2</sub>O), sodium borohydride (NaBH<sub>4</sub>), cetyltrimethylammonium chloride (CTA-Cl), ascorbic acid (AA), and silver nitrate (AgNO<sub>3</sub>) were purchased from Sigma-Aldrich. Cetyltrimethylammonium bromide (CTA-Br) was purchased from Fluka. All solutions were prepared with Nanopure water (resistivity 18.2 MΩ·cm) obtained from a Barnstead NANOpure DIwater system.

**2.2. Preparation Procedure of Gold Nanorods.** The nanorods were prepared through a seed-mediated procedure.<sup>31</sup> This procedure involves two main steps. (a) Preparation of gold seeds. Gold seed solution was prepared by first combining HAuCl<sub>4</sub> solution (5 mL, 0.5 mM) and CTA-Br (5 mL, 0.2 M), followed by addition of freshly made NaBH<sub>4</sub> solution (0.6 mL, 10 mM) under vigorous stirring. After ~5 min, magnetic stirring was stopped, and the as-prepared seed solution was further aged for several hours prior to nanorod preparation. (b) Preparation of Au nanorods. Growth solution consists of HAuCl<sub>4</sub> (final concentration 0.5 mM), CTA-Br (0.1 M), and AgNO<sub>3</sub> (0.12 mM). Ascorbic acid (105 μL of 0.1 M solution) was then added, followed by brief stirring (~1 min). Lastly, 25 μL of the seed solution was added to the growth solution (with brief stirring to homogenize the solution). The solution was left to stand on bench and sampled in different time intervals for UV–vis spectroscopic analysis.

**2.3. Characterizations.** UV–vis absorption spectra (190–1100 nm) were recorded using a Hewlett-Packard (HP) 8453 diode array spectrophotometer. Transmission electron microscopy (TEM) imaging was performed on a Hitachi 7100 TEM operated at 75 kV. HR-TEM is performed on a FEI G-20 microscope operated at 200 kV.

## 3. Results and Discussion

The standard seeding growth of Au nanorods involves two steps: (1) the preparation of small Au seeds and (2) the seeding growth of Au nanorods in the presence of CTA-Br and AgNO<sub>3</sub>. Our studies focus on the second step, in particular, the potential role of CTA<sup>+</sup> and Br<sup>-</sup>.

**3.1. Effect of CTA-Br Concentration of the Growth Solution.** We first varied the concentration of CTA-Br in the growth solution while keeping all the other experimental conditions the same as in the standard protocol. Figure 1A shows the UV–vis spectra of final Au nanoparticles for different CTA-Br concentrations (i.e., 0.1, 0.06, and 0.02 M). Note that the standard

(30) Jana, N. R.; Gearheart, L.; Murphy, C. J. *J. Phys. Chem. B* **2001**, *105*, 4065–4067.

(31) Nikoobakht, B.; El-Sayed, M. A. *Chem. Mater.* **2003**, *15*, 1957–1962.

(32) Murphy, C. J.; San, T. K.; Gole, A. M.; Orendorff, C. J.; Gao, J. X.; Gou, L.; Hunyadi, S. E.; Li, T. *J. Phys. Chem. B* **2005**, *109*, 13857–13870.

(33) Wei, Z.; Zamborin, F. P. *Langmuir* **2004**, *20*, 11301–11304.

(34) Johnson, C. J.; Dujardin, E.; Davis, S. A.; Murphy, C. J.; Mann, S. *J. Mater. Chem.* **2002**, *12*, 1765–1770.

(35) Liu, M. Z.; Guyot-Sionnest, P. *J. Phys. Chem. B* **2005**, *109*, 22192–22200.

(36) Smith, D. K.; Korgel, B. A. *Langmuir* **2008**, *24*, 644–649.

(37) Lofton, C.; Sigmund, W. *Adv. Funct. Mater.* **2005**, *15*, 1197–1208.

(38) Perez-Juste, J.; Liz-Marzan, L. M.; Carnie, S.; Chan, D. Y. C.; Mulvaney, P. *Adv. Funct. Mater.* **2004**, *14*, 571–579.

(39) Sau, T. K.; Murphy, C. J. *Philos. Mag.* **2007**, *87*, 2143–2158.

(40) Filankembo, A.; Giorgio, S.; Lisiecki, I.; Pileni, M.-P. *J. Phys. Chem. B* **2003**, *107*, 7492–7500.

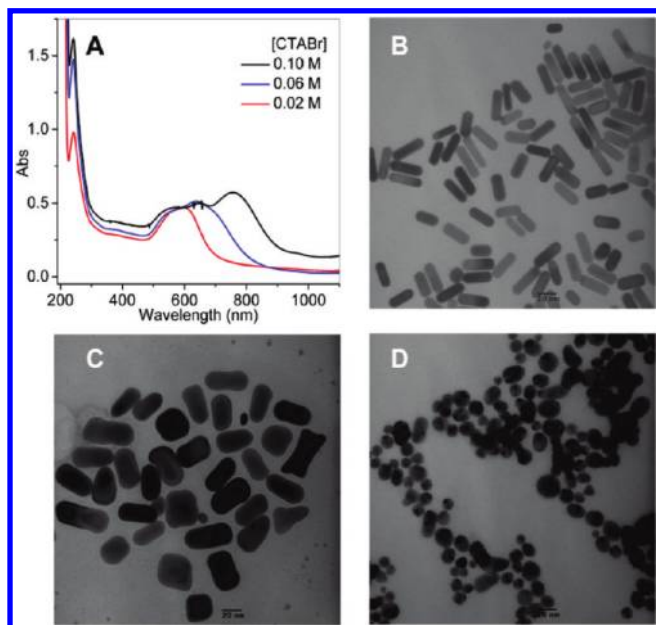


**Figure 1.** (A) UV-vis spectra of gold nanoparticles formed under different concentrations of CTA-Br in the growth solution. (B–D) TEM images corresponding to CTA-Br concentration of 0.1 M (B), 0.06 M (C), and 0.02 M (D). Scale bars are 20 nm.

CTA-Br concentration is 0.1 M. We found that the 0.1 M CTABr concentration is necessary in order to effect the growth of Au nanorods with the typical aspect ratio ( $AR \sim 3.5$ ); these nanorods exhibit a longitudinal SPR mode at  $\sim 800$  nm (Figure 1A). TEM confirms the morphology of the resultant nanorods (Figure 1B), which typically have a diameter of  $\sim 10$  nm and length of  $\sim 35$  nm.

When the CTABr concentration is lower, e.g. 0.06 M, the longitudinal SPR peak appears at significantly shorter wavelength ( $\sim 630$  nm) compared to the standard case ( $\sim 800$  nm) (Figure 1A). TEM analysis shows that the resultant Au nanorods are much larger in diameter ( $\sim 25$  nm) while the length is  $\sim 40$  nm (Figure 1C). When the CTABr concentration is further decreased to 0.02 M, only spherical (or slightly prolate) nanoparticles were produced (Figure 1D) with the SPR peak at  $\sim 585$  nm.

These results indicate the importance of CTA-Br concentration for the formation of typical Au nanorods. When the CTA-Br concentration is lower than 0.1 M, particle growth along the *radial* direction (or side growth) also occurs to a considerable degree. Thus, CTA-Br plays a major role in *inhibiting* the side growth during the elongation or 1D growth of nanorods. Lower concentrations of CTA-Br apparently cannot sufficiently inhibit the side growth of nanorods. Previous work by Murphy et al. suggests that the nanorod side faces are protected by a CTA<sup>+</sup> bilayer (i.e., rod-shaped micelles).<sup>32</sup> On the basis of the above observations and literature work, several questions naturally arise: (1) Is the high concentration (0.1 M) of CTA<sup>+</sup> cations needed for micelle formation? (2) Are the high concentrations (0.1 M) of both CTA<sup>+</sup> and Br<sup>-</sup> needed for rod formation? (3) Does the anion (Br<sup>-</sup>) matter in the nanorod formation? These questions motivated us to pursue a more systematic study on the nanorod growth process. It is worth noting that previous literature work has determined the cmc of CTA-Br to be  $\sim 1$  mM;<sup>41</sup> this is significantly lower than the used CTA-Br concentration for Au nanorod growth. Therefore, we suspect that the anion (Br<sup>-</sup>) in CTA-Br perhaps has some important role in the seeding growth

process of Au nanorods. Below we design various sets of experiments to gain insight into the role of Br<sup>-</sup> ions.

**3.2. Effect of the Nature of Halide Ions in Growth Solution.** We first replace Br<sup>-</sup> with Cl<sup>-</sup> by using CTA-Cl but keep the total concentration of CTA<sup>+</sup> cations constant ( $\sim 0.1$  M) in the growth solution. This experiment allows to probe the role of the counterion of the surfactant while keeping the CTA<sup>+</sup> micelles essentially unaltered since the micellar structure is primarily determined by CTA<sup>+</sup> rather than by X<sup>-</sup>.

We investigated Br<sup>-</sup>/Cl<sup>-</sup> ratios of 2:1, 1:1, and 1:2 (in the order of decreasing Br<sup>-</sup> concentration). Interestingly, in all cases of mixed halide ions (total 0.1 M) the distinct longitudinal SPR peak at  $\sim 800$  nm disappeared, indicating that *none* of these conditions result in typical Au nanorods of similar aspect ratio as those formed under *sole* CTABr (0.1 M) condition (Figure 2A). TEM analysis shows that under the Br<sup>-</sup>/Cl<sup>-</sup> ratios of both 0.066 M/0.033 M (2:1) and 0.05 M/0.05 M (1:1), a mixture of nanorods (predominant), some spherical particles and nanocubes, is formed (Figure 2B). The nanorods show a somewhat larger diameter ( $\sim 15$  nm vs  $\sim 10$  nm in *sole* CTABr condition) and a shorter length ( $\sim 30$  nm), indicating a side growth of nanorods occurs as well. This is consistent with the case of lowering CTA-Br concentration (cf. 0.06 M, Figure 1C), indicating that Cl<sup>-</sup> ions are less efficient in inhibiting radial growth of nanorods than do Br<sup>-</sup> ions. In the case of 1:2 ratio of Br<sup>-</sup>/Cl<sup>-</sup>, the aspect ratio and yield of nanorods are even lower. These results clearly demonstrate that Br<sup>-</sup> ions play a major role in Au nanorod formation and that higher anisotropy is only obtained in the presence of sufficient bromide in the growth solution.

The above observations led to an interesting question of whether other Br<sup>-</sup> sources (e.g., NaBr) can effect Au nanorod growth. Below we perform experiments to investigate this. Of note, we did not pursue I<sup>-</sup> ions as they strongly bind to Au and seem to destroy particles.

**3.3. Effect of Bromide Ions from an External Source.** To further investigate the role of Br<sup>-</sup>, we intentionally used a low concentration of CTABr (0.02 M), at which Au nanorods do not form (see Figure 1D). Under this condition, we added various amounts of NaBr to the growth solution to investigate the effect of extrinsic Br<sup>-</sup> ions (as opposed to intrinsic Br<sup>-</sup> from CTABr). Surprisingly, we found that the addition of NaBr indeed effects the growth of nanorods and that the anisotropy of Au nanorods improves with increasing concentration of NaBr from 0.02 to 0.08 M (Figure 3). The nanorods formed under NaBr (0.08 M) and CTABr (0.02 M) have an average diameter of  $\sim 15$  nm and a length of  $\sim 35$  nm. Note that higher NaBr concentrations ( $> 0.08$  M) were not investigated.

These results explicitly demonstrate that externally added bromide in the form of NaBr can indeed lead to effective growth of nanorods, even when the CTABr concentration is not sufficient (e.g., 0.02 M) for Au nanorod formation. Therefore, in the case of standard conditions for nanorod growth, i.e. with *sole* CTABr (0.1 M), the anion (Br<sup>-</sup>) should play a more significant role than does the CTA<sup>+</sup> cation in terms of directing the rod shape, for that CTABr only (e.g., 0.02 M) cannot effect nanorod growth (Figure 1D).

**3.4. Effect of CTA-Br below Critical Micelle Concentration.** The afore-discussed results show that bromide ions play a critical in effecting anisotropy of Au nanoparticles in the seeded growth process. To gain more information, we further attempted to prepare Au nanorods with growth solutions containing very low concentrations of CTABr (even below its cmc value  $\sim 1$  mM), but the total bromide concentration in the growth solution is still maintained at 0.1 M by adding NaBr. This set of experiments is

(41) Huang, X.; Yang, J.; Zhang, W.; Zhang, Z.; An, Z. *J. Chem. Educ.* **1999**, *76*, 93–94.

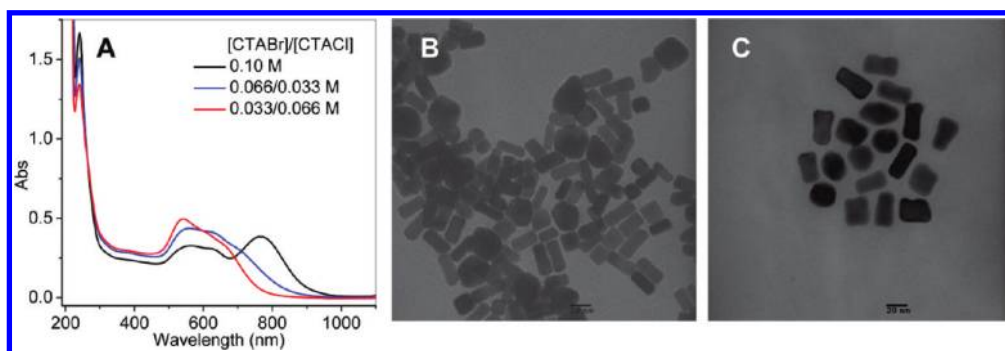


**Figure 2.** (A) UV-vis spectra of Au nanoparticles formed under different ratios of CTABr/CTACl. (B) TEM image of nanoparticles formed at 0.066 M/0.033 M and (C) 0.033 M/0.066 M. Scale bars are 20 nm.

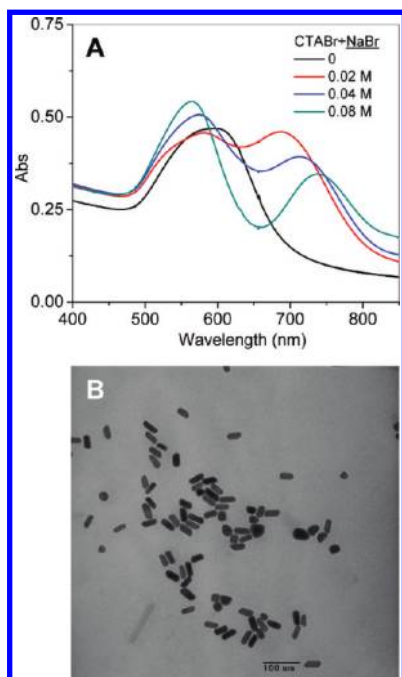


**Figure 3.** (A) UV-vis spectra of Au nanoparticles corresponding to growth solutions containing CTABr (0.02 M, same for all the solutions) and 0, 0.02, 0.04, and 0.08 M NaBr, respectively. (B) TEM image of Au nanoparticles for the condition of CTABr (0.02 M) mixed with NaBr (0.08 M).

designed to evaluate how important the  $\text{CTA}^+$  micelle is for Au nanorod formation.

We have varied the CTABr concentration from 3.0 mM down to 0.5 mM; note that 0.5 mM is already below the cmc value. The results show that, in all cases, Au nanorods are predominantly formed (Figure 4). The nanorods have typical dimensions of diameter  $\sim 15$  nm and length  $\sim 40$  nm. Even when the CTABr concentration (0.5 mM) is below its cmc (1 mM), nanorods are still formed (Figure 4B), albeit with a lower yield. These experiments clearly show that, as long as sufficient  $\text{Br}^-$  ions exist in the growth solution, the growth of nanorods can take place even when  $\text{CTA}^+$  concentration is below its cmc value.

When the concentration of CTABr is at its cmc value of  $\sim 1$  mM, under which nanorods are predominantly formed, we further investigated the effect of adding increasing amounts of NaBr to the growth solution to determine the optimal NaBr concentration for nanorod growth. Figure 5 shows that anisotropy is gained at an optimal  $[\text{Br}^-]$  concentration range of 0.05–0.10 M.

**3.5. Discussions.** Taken together, the above results clearly demonstrate the important role of  $\text{Br}^-$  in the seeding growth of Au

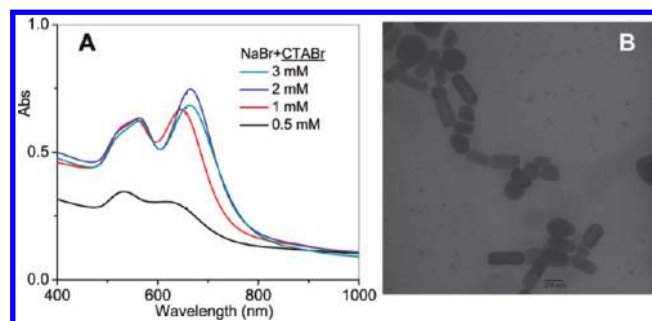


**Figure 4.** (A) UV-vis spectra of Au nanoparticles formed under low concentrations (mM) of CTABr; the total  $[\text{Br}^-]$  is fixed at 0.1 M. (B) TEM image of Au nanoparticles corresponding to 0.5 mM CTABr and 99.5 mM NaBr.

nanorods. It is worth noting that Sau and Murphy also pointed out the important role of anions in the surfactants used in the synthesis of gold nanorods and nanowires.<sup>39</sup> In the CTABr-effected growth process (standard procedure), the  $\text{CTA}^+$  cations provide steric protection of the nanorods; our results show that its concentration could be decreased to its cmc value. Thus, the high concentration of  $\text{CTA}^+$  (0.1 M) in the standard protocol is not necessary for Au nanorod formation; albeit a minimum amount of  $\text{CTA}^+$  is still needed for protecting Au nanorods since the surface-bound bromide species do not offer steric protection. Below we focus on the discussion of the role of  $\text{Br}^-$  ions based upon our observations.

Previous work has shown that halide ions interact with gold surfaces, and the interaction strength follows the increasing order of  $\text{F}^- < \text{Cl}^- < \text{Br}^- < \text{I}^-$ , which reflects the decreasing energy of solvation of these ions.<sup>40</sup> Among the halides,  $\text{F}^-$  ions nonspecifically adsorb to gold surface;  $\text{Cl}^-$  ions also bind to gold via a weak interaction, while  $\text{I}^-$  ions bind too strongly to gold surface and tend to destroy Au nanoparticles. Indeed, recent work by Korgel and co-workers demonstrated that a very low concentration ( $\sim$  ppm) of  $\text{I}^-$  impurity in CTABr prevents nanorod growth.<sup>18</sup> Thus, only  $\text{Br}^-$  is left as a suitable candidate since it binds to gold not *too weakly nor too strongly*. Our results of replacing  $\text{Br}^-$  ions partially with  $\text{Cl}^-$  ions (see section 3.2) clearly show their difference in inhibiting radial growth of Au nanorods. We believe that such an intermediate binding capability of  $\text{Br}^-$  is one of the key characters that  $\text{Br}^-$  ions can effect the growth of Au nanorods. Of note, bromide was also found to promote anisotropic growth in the synthesis of Pd nanobars and nanorods.<sup>4</sup> An interesting question is how  $\text{Br}^-$  ions effect the 1D growth of Au nanoparticles. Previous work by Murphy et al.<sup>32</sup> studied the structure of Au nanorods using HR-TEM. The Au nanorods adopt a penta-twinned structure, and the two ends are enclosed by  $\{111\}$  facets while the rod sides are bound by  $\{110\}$  (and  $\{100\}$  if

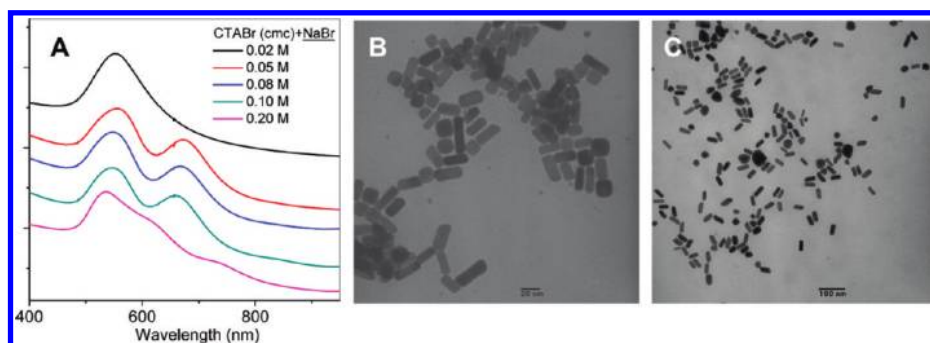


**Figure 5.** (A) UV–vis spectra resulting from supplementing the bromide concentration of growth solutions containing 1 mM CTABr with NaBr. TEM images for conditions of (B) 0.05 M NaBr and (C) 0.08 M NaBr.

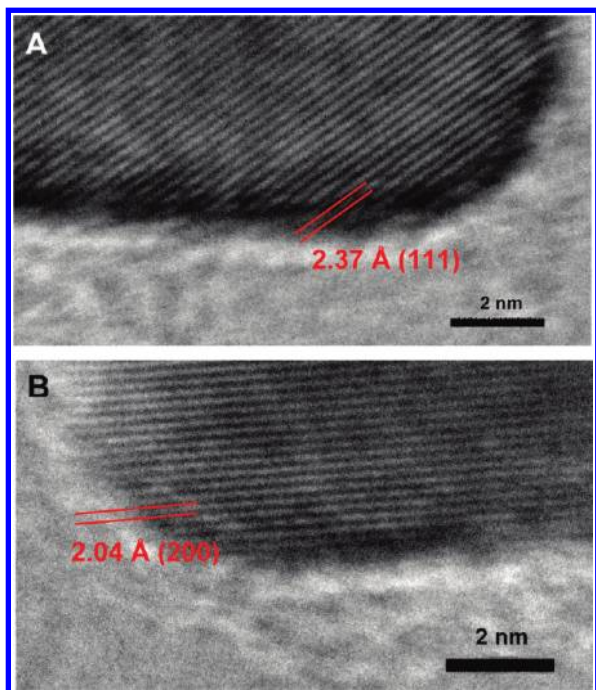


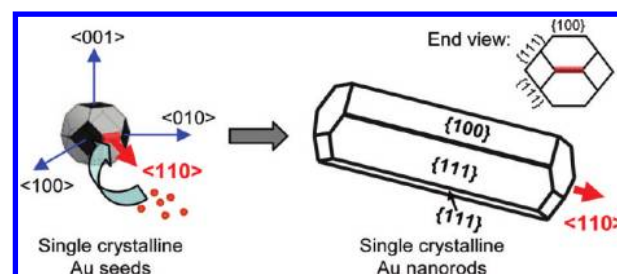
**Figure 6.** HR-TEM of Au nanorods effected by NaBr in the presence of minimal CTABr.

truncation occurs. In this structure, the top and bottom ends of nanorods form a decahedron fully enclosed by ten  $\{111\}$  facets. The central axis of a decahedron is parallel with the  $[110]$  direction; thus, penta-twinned Au nanorods grow along the  $[110]$  direction. However, Liu and Guyot-Sionnest found the nanorod structure depends on the seeds used.<sup>35</sup> If CTABr protected Au seeds, rather than citrate protected seeds, are used in the growth process, single crystalline (as opposed to penta-twinned) nanorods are produced.

Herein, we employ HR-TEM to investigate the structure of NaBr-effected Au nanorods. Under HR-TEM, we randomly chose nanorods for both HR-TEM and electron diffraction analysis. In all the nanorods chosen for analysis, we did not find structural faults, indicating that the nanorods are all perfectly fcc single-crystalline rather than penta-twinned rods. Among the randomly chosen nanorods,  $(111)$  planes are predominantly observed (Figure 6A); the observed lattice spacing 2.37 Å is in excellent agreement with bulk Au  $(111)$  spacing (2.35 Å). When the rod is rotated,  $(200)$  lattices were seen (spacing: 2.05 Å, bulk Au  $(200) = 2.04$  Å) (Figure 6B).

Based upon the HR-TEM results, a structural model is constructed for the nanorod (Scheme 1). In this model, the side faces

**Scheme 1. Structural Model of Single Crystalline Au Nanorod and Proposed Growth Mechanism**



consist of four  $\{111\}$  facets and two  $\{100\}$  facets; note that the two  $\{100\}$  facets are due to longitudinal truncation (otherwise, the four  $\{111\}$  planes form a parallelogonal radial cross section of rod); this truncation is better observed from the end view of the rod (Scheme 1). Apparently, the nanorod growth direction is along  $[110]$ . The preferred growth of  $[110]$  nanorods, as opposed to  $[100]$  or  $[111]$  nanorods, is indeed energetically favorable according to the theoretical calculations by Barnard and Curtiss.<sup>45</sup>

We propose a mechanism for the seeding growth of  $[110]$  oriented, single crystalline Au nanorods. The starting Au seeds are typically quasi-spherical particles ( $\sim 2$  nm) based on TEM analysis. Such quasi-spherical particles are usually enclosed by low-index  $\{111\}$  and  $\{100\}$  facets; note that  $\{111\}$  facets possess the lowest surface energy (hence, the most stable type of facet) among the three types of low-index facets, and the  $\{110\}$  facets have the highest surface energy and hence are not preferentially exposed in quasi-spherical nanoparticles; the  $\{100\}$  facets are in between in terms of surface energy. We believe that one of the major roles of  $\text{Br}^-$  ions in the nanorod growth process is their etching interaction with the Au seeds. This chemical etching process leads to small single crystalline, polyhedral particles at the early stage of the growth process (Scheme 1), while those twinned particles may be dissolved due to  $\text{Br}^-$  etching. Apparently, this etching process occurs much easier on smaller seeds. This explains the relatively higher yield of nanorods using small Au seeds (e.g.,  $< 4$  nm);<sup>34</sup> in contrast, when one uses large nanoparticles (e.g., citrate stabilized  $\sim 10$ – $20$  nm Au particles) as seeds, Au nanorods are still formed but with much lower yield; this is because large particles are more difficult to be etched by  $\text{Br}^-$  to form the right type of polyhedral seeds for rod growth. Direct evidence of seed etching by  $\text{Br}^-$  will be pursued in our ongoing work. Since the  $\{111\}$  and  $\{100\}$  facets are more stable than  $\{110\}$ , it is reasonable to expect that the single crystalline seeds preferentially elongate along the  $[110]$  direction to maximize  $\{111\}$  facets (see the red highlighted  $(110)$  facet in Scheme 1).

From our observation that a minimal amount of CTABr ( $\sim$ sub-cmc concentration) is still needed for nanorod growth,

we believe that CTA<sup>+</sup> mainly provides a steric protection of the formed nanorods, albeit its templating role cannot be completely eliminated at this point. The  $\langle 110 \rangle$  elongation of the single crystalline seeds results in  $\{111\}$  and  $\{100\}$  side facets (Scheme 1). Subsequent passivation of side facets by Br<sup>-</sup> retards the radial (or side) growth and facilitates further elongation along the  $[110]$  direction. We speculate that Br<sup>-</sup> ions are adsorbed onto the  $\{100\}$  and  $\{111\}$  side facets by forming covalent bonds similar to Au–Br–Au bridging motifs. Such a bridging mode was observed in the crystal structure of ultrasmall 25-atom (Au<sub>25</sub>) nanorods.<sup>42,43</sup>

Previous work by Murphy and others has demonstrated that Au nanorods are stabilized by the CTA<sup>+</sup> bilayers.<sup>30,31</sup> Thus, both the CTA<sup>+</sup> bilayer and Br<sup>-</sup> are believed to be present on the side facets of nanorods. Both CTA<sup>+</sup> and Br<sup>-</sup> interact with nanorod side surfaces and significantly slow down the radial growth rate of nanorods, while the two ends are still subject to grow at a faster rate than the side facets, hence effecting anisotropic growth and leading to nanorods. With respect to the adsorption energy of CTA<sup>+</sup> on Au $\{hkl\}$  faces, theoretical calculations show that the CTA<sup>+</sup>/ $(111)$  system is more favored (interaction energy = -216 kcal/mol) than CTA<sup>+</sup>/ $(110)$  (-134 kcal) and CTA<sup>+</sup>/ $(100)$  (-132 kcal).<sup>44</sup> One may argue that  $\{111\}$  and  $\{100\}$  facets are emerged on the two ends of the nanorod as well (Scheme 1, end view), and hence, anisotropic growth seems not to be favored. However, one should realize that the CTA<sup>+</sup> bilayer forms an ordered and dense layer on the regular side facets but is disordered on the two ends of nanorod due to high curvature of the ends; this leads to preferential deposition of reduced Au atoms onto the two ends. Taken together, this quasi-1D anisotropic growth eventually leads to well-defined nanorods with their aspect ratio controllable by controlling the experimental conditions.

There are certainly many details to be elucidated in the above proposed growth mechanism. One of the important aspects is the specific role of Ag<sup>+</sup> in the Au nanorod growth process. The addition of AgNO<sub>3</sub> to the CTABr-containing growth solutions leads to immediate formation of AgBr, but the cloudy AgBr soon disappears due to conversion to AgBr<sub>2</sub><sup>-</sup> since Br<sup>-</sup> is in large

excess. In the literature, it has been hypothesized that Ag<sup>+</sup> ions form an adsorbate layer on the Au particle surface in the form of AgBr, which restricts radial growth of rods. The valence state of silver is under debate: Some work indicates that silver ions are not reduced to Ag(0) during rod growth, but Liu and Guyot-Sionnest suggested an underpotential deposition of Ag(0) on the different crystal facets of gold, leading to symmetry-breaking and rod formation.<sup>35</sup> The role of Ag(I) and its exact form on the surface of nanorods remains to be elucidated in future work.

#### 4. Conclusion

This work identifies the important role of Br<sup>-</sup> as a shape-directing agent in the seed-mediated growth of Au nanorods. CTABr plays a major role in *inhibiting* the side growth during the elongation of nanorods. The previously thought picture of Au nanorod formation is that nanorods were effected by rodlike micelles of CTA-Br surfactants. If the micelle-directed growth mechanism dominates the process, when the CTABr concentration is below its cmc value, one should not obtain Au nanorods in high yield. However, our results show that even when the CTABr concentration is below cmc, one can still obtain Au nanorods in good yield by remediating the Br<sup>-</sup> concentration by adding NaBr. Thus, a high concentration of Br<sup>-</sup> ions, rather than of CTA<sup>+</sup>, is indeed necessary to effect nanorod growth. For CTA<sup>+</sup>, only a minimal concentration is needed to provide steric protection of the formed nanorods. Thus, Br<sup>-</sup> ions are more critical for Au nanorod formation than CTA<sup>+</sup>. The rod shape and dimensions of the resulting Au nanorods are readily controllable by the concentration of Br<sup>-</sup> ions. High-resolution TEM studies show that the as-formed nanorods are perfectly fcc single crystalline, in contrast with the penta-twinned rods reported previously. The side faces of the nanorod are found to consist of  $\{111\}$  and  $\{100\}$  facets, and the nanorod growth direction is along  $[110]$ . A mechanism is proposed to account for the roles of bromide ions in seeding growth of Au nanorods, including (1) etching to form single crystalline faceted seeds and eliminating twinned seeds and (2) surface passivation of  $\{111\}$  and  $\{100\}$  facets of nanorods together with CTA<sup>+</sup> bilayers. This work clearly demonstrates that the Br<sup>-</sup> ions indeed serve as a shape-directing agent for synthesizing gold nanorods.

**Acknowledgment.** We thank Dr. N. Thomas Nuhfer for assistance with HR-TEM. This work is supported by CMU, AFOSR, and NIOSH.

(42) Shichibu, Y.; Negishi, Y.; Watanabe, T.; Chaki, N. K.; Kawaguchi, H.; Tsukuda, T. *J. Phys. Chem. C* **2007**, *111*, 7845–7847.

(43) Qian, H.; Zhu, M.; Lanni, E.; Zhu, Y.; Bier, M. E.; Jin, R. *J. Phys. Chem. C* **2009**, *113*, 17599–17603.

(44) Bai, X.; Gao, Y.; Liu, H.; Zheng, L. *J. Phys. Chem. C* **2009**, *113*, 17730–17736.

(45) Barnard, A. S.; Curtiss, L. A. *J. Mater. Chem.* **2007**, *17*, 3315–3323.